

# Simulations show tumor vascular morphology affects the accuracy of steady-state susceptibility contrast MRI biomarkers of angiogenesis

Eugene Kim<sup>1</sup>, B. Douglas Ward<sup>2</sup>, and Arvind P. Pathak<sup>3</sup>

<sup>1</sup>Department of Biomedical Engineering, Johns Hopkins University, Baltimore, MD, United States, <sup>2</sup>Department of Biophysics, Medical College of Wisconsin, Milwaukee, WI, United States, <sup>3</sup>Russell H. Morgan Department of Radiology and Radiological Science, The Johns Hopkins University School of Medicine, Baltimore, MD, United States

**Target Audience:** This work is targeted toward preclinical and clinical researchers using steady-state susceptibility contrast (SSC)-MRI biomarkers to assess *in vivo* tumor angiogenesis.

**Purpose:** SSC-MRI biomarkers such as fractional blood volume (FBV) <sup>1</sup>, vessel size index (VSI) <sup>1</sup>, and vessel density (N) <sup>2</sup> are often used to assess angiogenesis and response to anti-angiogenic therapy in preclinical and clinical tumors. These biomarkers are theoretically derived from an infinite cylinder model (ICM), i.e. blood vessels are modeled as an ensemble of randomly oriented, infinitely long cylinders. However, actual tumor vessels are tortuous, chaotic and deviate from the ICM. Here, we determine *in silico* the effect of real tumor vascular geometry on the accuracy of these biomarkers.

**Methods:** Three angiogenic biomarkers (FBV, VSI, N) were computed *in silico* for two scenarios: (i) the real 3D vasculature derived from micro-CT ( $\mu$ CT) images of an MDA-MB-231 human breast cancer xenograft, and (ii) an ensemble of randomly oriented cylinders (RC) with similar vascular volume fraction (~2%) and cylinder (vessel) radius distribution ( $6.5 \pm 3.4 \mu\text{m}$ ) as the tumor. Briefly, MDA-MB-231 human breast cancer cells were orthotopically inoculated into the mammary fat pad of a female nude mouse. Five weeks after inoculation, the mouse was perfused with Microfil<sup>®</sup> (Flow Tech Inc., Carver, MA) and the tumor excised for *ex vivo*  $\mu$ CT angiography (Numira Biosciences Inc., Salt Lake City, UT). The 3D tumor vasculature was segmented from the  $\mu$ CT image and used to compute ground truth FBV, VSI, and vessel density maps (Fig. 1b-d). The finite perturber method (FPM) <sup>3</sup> was then used to approximate magnetic field perturbations ( $\Delta B$ ) created by a super-paramagnetic contrast agent inside the tumor vasculature (Fig. 1a), which was incorporated into Monte Carlo simulations to generate SSC-MRI multi-echo spin echo (SE) and gradient echo (GE) images (matrix= $64 \times 64 \times 4$ , voxel size= $220 \times 220 \times 250 \mu\text{m}^3$ ) (Fig. 1e). The simulated SE and GE signal time courses were fitted to a mono-exponential model to compute  $\Delta R_2$  and  $\Delta R_2^*$  maps from which *in silico* FBV, VSI, and N maps were computed (Fig. 1f-h). The same procedure was applied to the RC ensemble and corresponding ground truth FBV, VSI, and vessel density maps computed. Tumor vessel and RC simulations were conducted at pre-clinical (9.4T) and clinical (1.5T) field strengths. For each scenario, the two-tailed Wilcoxon signed-rank test was used to determine whether the voxel-wise errors between simulated FBV and VSI values and their corresponding ground truth values were significantly different ( $\alpha = 0.001$ ) for different field strengths. The Mann-Whitney U test was used to determine if these errors differed significantly between the tumor and RC data. Finally, for each scenario the Fisher transformation and two-tailed  $p$ -value ( $\alpha = 0.05$ ) were used to compare voxel-wise Pearson correlation coefficients between the simulated and ground truth values of the three angiogenic biomarkers.

**Results:** Comparing the  $\mu$ CT to the RC data, the correlations between ground truth and simulated values were significantly higher for FBV and significantly lower for VSI and N (Table 1), while the median errors in simulated FBV and VSI were significantly larger (Fig. 2). For both  $\mu$ CT and RC data, the FBV and VSI correlations were higher at 1.5T than 9.4T, but the median errors of the *in silico* FBV and VSI measurements were also larger at the lower field. These differences were not significant for the RC data, while all but the difference in FBV correlation were significant for the  $\mu$ CT data. In contrast, the correlation between N and vessel density was significantly lower at 1.5T than 9.4T for both datasets.

**Discussion:** These results indicate that tumor vascular morphology adversely affects the accuracy of SSC-MRI angiogenic biomarkers. Consistent with previous studies, simulated FBV and VSI overestimate the true blood volume and vessel size. The systematic errors in simulated FBV and VSI measurements suggest that these parameters may not be suitable for making absolute measurements *in vivo*, particularly at clinical field strengths where the theoretical model assumptions (e.g. being in the static dephasing regime) may not hold. For FBV, however, simulated and true values were highly correlated at both field strengths. The higher correlation for the  $\mu$ CT data than for the RC data may be due to the  $\mu$ CT dataset having a larger range of FBV values created by the high spatial heterogeneity found in tumors. This strong correlation suggests that  $\Delta R_2^*$  ( $\propto$ FBV) is suitable as a pre-clinical and clinical measure of relative blood volume. Similarly, for the tumor vasculature, *in silico* values of relative measures of vessel size (i.e.  $\Delta R_2^*/\Delta R_2$ ) and vessel density (i.e.  $\Delta R_2/(\Delta R_2^*)^{2/3}$ ) exhibited significantly higher correlations with true values compared to VSI and N, with the exception of  $\Delta R_2^*/\Delta R_2$  at 9.4T (Table 1).

**Conclusion:** Using an *in silico* approach, we demonstrated that the ICM assumptions made in deriving the expressions for FBV, VSI, and N may not be valid for real tumor vascular networks. The computational methods described here may be applied to elucidate the effects of vessel geometry, magnetic field strength, contrast agent dose, diffusion, and other biophysical factors on the SSC-MRI signal to develop more accurate clinical *in vivo* biomarkers of angiogenesis.

**Table 1** Pearson correlation coefficients between ground truth and *in silico* values

	FBV		VSI ( $\Delta R_2^*/\Delta R_2$ )		N ( $\Delta R_2/(\Delta R_2^*)^{2/3}$ )	
	1.5T	9.4T	1.5T	9.4T	1.5T	9.4T
Random cylinders	0.68	0.62	0.64	0.50	0.48*	0.65
Tumor vasculature	0.89	0.88	0.35*	-0.14	0.29*	0.33
			(0.46)*	(-0.08)	(0.60)*	(0.66)

\* Correlation coefficient is significantly different at 1.5T than 9.4T ( $P < 0.05$ ).

**References:** 1. Tropèrès I, Grimault S, Vaeth A, et al. Vessel size imaging. *Magn Reson Med.* 2001; 45(3):397-408. 2. Jensen JH, Chandra R. MR imaging of microvasculature. *Magn Reson Med.* 2000; 44(2):224-30. 3. Pathak AP, Ward BD, Schmainda KM. A novel technique for modeling susceptibility-based contrast mechanisms for arbitrary microvascular geometries: the finite perturber method. *Neuroimage.* 2008; 40(3):1130-43.

**Acknowledgements:** Research supported by Komen Foundation Grant KG090640

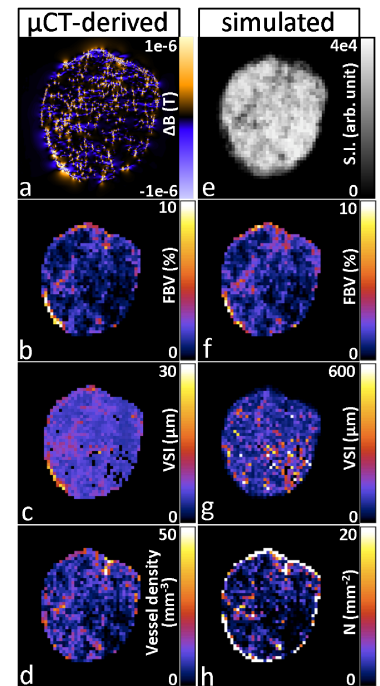


**Fig. 1** (a) Magnetic field perturbation  $\Delta B$  created by a 1 mm thick section of real,  $\mu$ CT-derived tumor vasculature with a susceptibility difference  $\Delta\chi = 0.112$  ppm (c.g.s units) and  $B_0 = 9.4\text{T}$ . Corresponding FBV (b), VSI (c), and vessel density (d) maps computed directly from the tumor vasculature. (e) Simulated GE ( $TE = 20$  ms) image of the same tumor slice. Maps of FBV (f), VSI (g), and N (h) computed from the simulated MR signal.

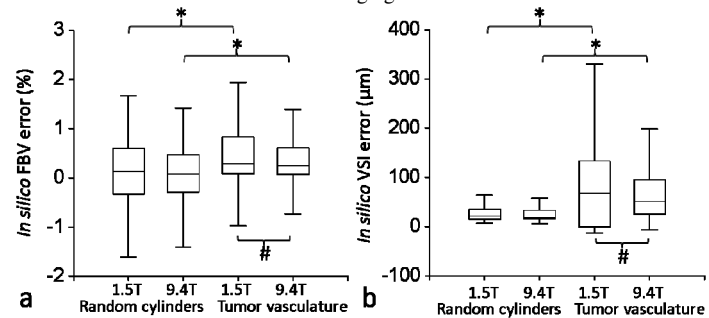


**Fig. 2** Box plots of the voxel-wise errors in simulated FBV (a) and VSI (b) measurements. Outliers are not shown. Non-parametric two-sample (\*) or paired (#) test shows median errors are significantly different ( $P < 0.001$ ):